MACROSCOPIC EVALUATION OF INCIDENT-INDUCED DRIVER BEHAVIOR CHANGES

Ziaur Rahman
Graduate Teaching Assistant
Department of Civil Engineering
University of Texas at Arlington
P.O. Box 19308
Arlington, TX 76019-0308
Phone: (817) 272-0251
E-mail: Ziaur.rahman@mavs.uta.edu

Stephen P. Mattingly
Associate Professor (Corresponding author)
Department of Civil Engineering
University of Texas at Arlington
P.O. Box 19308
Arlington, TX 76019-0308
Phone: (817) 272-2859, Fax: (817) 272-2630
E-mail: mattingly@uta.edu

ABSTRACT

Reducing the impact of incidents on the freeway network, which represents a key goal for most regional traffic management systems, requires an effective traffic incident management system. Early and accurate recognition of incident impact the network represents one of the key challenges associated with incident management. Microscopic simulation represents an effective strategy for forecasting incident impact because it provides opportunities to study diverse conditions that may occur irregularly both spatially and temporally in the field. Oftentimes, the traffic simulation parameters appear be calibrated for uncongested conditions. This research explores macroscopic network performance when applying microscopic simulation models calibrated under both congested and uncongested conditions; the research considers a default uncongested parameter set and compares it with a parameter set calibrated using macroscopic data during congested conditions and a parameter set calibrated using microscopic data during congested conditions. Using a testbed along I-210 in Pasadena, California, the study varies incident duration, traffic volume and lane closures to investigate the change in results across all three models. The study also investigates six actual incidents and compares the simulation results with the observed field conditions collected from the California Department of Transportation Performance Measurement System database. During the experimental cases, the macroscopic congested parameter set consistently estimates longer network travel times and slower speeds. The comparison with the field conditions confirms that the macroscopic congested parameter set better reflects field performance especially during more congested conditions. This research indicates the need to use congested conditions for calibration when investigating incident impact.

1. INTRODUCTION

An effective traffic incident management system has a crucial impact on reducing or minimizing the impact of incidents on the freeway network; it represents one of the key goals for most regional traffic management systems. The blockage or closure of freeway lanes causes significant delays on the road network [Kwon *et al*., 2006]. These temporary blockages may cause changes in driving behavior in both blocked and unblocked lanes. As incidents create queues, delay, rubbernecking, secondary crashes and many other problems, the accurate assessment of incident impacts appears critical for effective operational management policies.

Microscopic traffic simulation provides opportunities to study diverse experimental traffic conditions that may occur irregularly both spatially and temporally in the field. Oftentimes, the parameters in the traffic simulation software appear to only be calibrated for the uncongested situation. Recent research (Gomes *et al*., 2004) indicates that microscopic traffic simulation parameters may actually change during incident conditions. Within the incident zone, which is where the lane numbers are reduced, Knoop *et al*. (2009) shows that the driver reaction time increases significantly and produces a thirty percent lower queue discharge rate at the macroscopic level. In this study, the researchers use traffic simulation to investigate the impact of incident induced changes in microscopic behavior parameters' on macroscopic performance.

Woody (2006) finds that the VISSIM parameters, CC0, CC1, CC2, CC4 and CC5, have more influence on the capacity of a freeway section than other parameters. Sheu (2006) models intra-lane and inter-lane traffic behavior. Sheu calibrates the microscopic travel behavior characteristics: maximum acceleration, maximum deceleration, minimum safety spacing, and mean reaction time. The current research integrates these four traffic behavior parameters in a VISSIM model and compares the network performance resulting from an incident when VISSIM is calibrated based on congested and uncongested conditions. The definition of maximum acceleration from Sheu's research is similar to the definition of driver behavior parameter CC9, which is actually acceleration at 50 mph. According to PTV VISION, the maximum deceleration is the maximum technically feasible deceleration. During an incident induced situation, driver behavior impacts both car-following and lane changing based on the minimum safety spacing and mean reaction time. The minimum safety spacing is similar to standstill distance, and mean reaction time is compared with CC1 (headway time). The study investigates the following research questions:

- What are the differences in macroscopic performance measures (such as speed, flow and delay) when congested freeway conditions are simulated using traffic behavior parameters calibrated under congested conditions versus those calibrated under uncongested conditions?
- Do the number of lanes blocked during an incident affect the magnitude of these differences?
- What effect, if any, does incident duration have on these differences?
- Does the amount of demand affect these differences?
- Do the uncongested-based parameters or the congested-based parameters more accurately reflect observed field performance during congested conditions?

2. METHODOLOGY

2.1. Test Environment

This paper considers a previously studied fifteen mile long section of I-210 West between Vernon St. and the SR-134 junction in Pasadena, California (Figure 1). This site is selected because it has both California Department of Transportation (Caltrans) Performance Measurement System (PeMS) data (e.g. speed, flow, and occupancy) and California Highway Patrol incident data available. Furthermore, an earlier study specifically calibrates VISSIM for this site using qualitative operational criteria during congested conditions (Gomes *et al.*, 2004). The current study uses PeMS data sources during both the experimental and validation phases of the project.

This freeway section has a High Occupancy Vehicle (HOV) lane, a freeway connector, and twenty metered on-ramps with and without bypass lanes. A median side HOV lane spans the entire study network and is separated by intermittent barrier. The Gomez *et al*. (2004) test network uses these characteristics to replicate the exact field conditions. However, the current study only considers the main lane movement of EB and WB I-210 because the study focuses on the car-following and lane changing behavior specifically related to an incident rather than allowing those resulting from weaving, merging and diverging to interfere. As a result, the study does not consider any HOV or on- and off-ramp movements. The research design treats HOV lanes as a regular lane with the main lane movement because the incident location of gives the drivers access to the HOV lane. Figure 1 shows the location of the study network in Los Angeles.

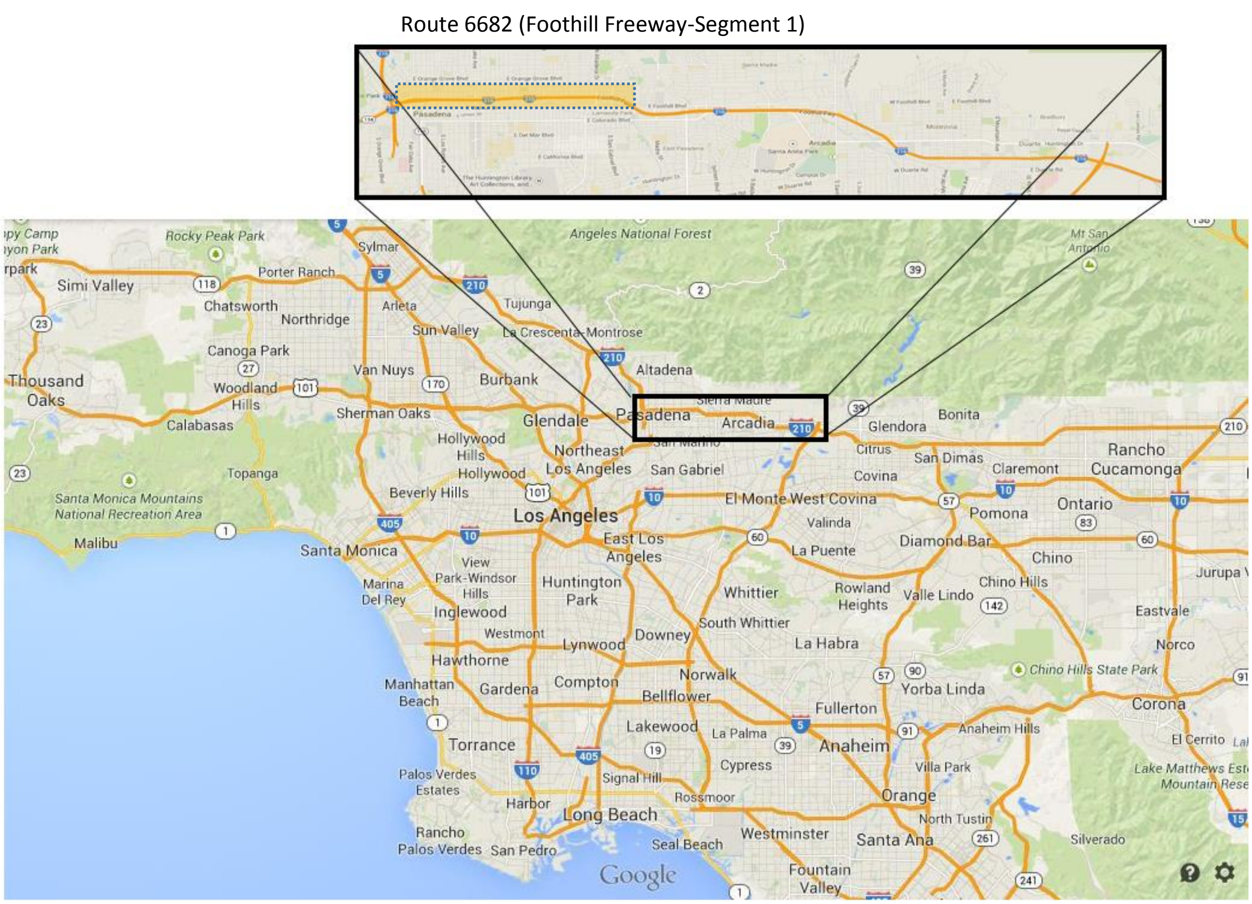

FIGURE 1 Geographic position of the study network (Google Map, Accessed on July 2014).

VISSIM simulations require a comprehensive and complete description of the network layout for a realistic output, and the recommended method for entering geometric information is to construct a scaled map, in a bitmap or jpeg format. Using thirty-two high resolution Google pictures from Google map, the author makes a single panorama view of the network with the ‘photo merge’ command of Adobe Photoshop. The research team uses the network graphic as the background for the VISSIM network. Important features for replicating the test bed include:

1. Number of lanes
2. Width of lanes
3. Lane drops
4. Auxiliary lanes
5. Location of the HOV lanes
6. Location of data collection points
7. Location of the experimental incident

TABLE 1 Layout of Study Network Sections

ID	Schematic	Start Name	CA PM	Abs PM	Length	Lanes+ HOV+ Auxilary	Auxilary Start	Auxilary End
717606		Orange Grove	R13.18	13.18	0.53	4+1+0	N/A	N/A
717631		Fair Oaks 1	R25.14	25.12	0.46	4+(1)+0	N/A	N/A
717633		Marengo	R25.74	25.72	0.68	5+1+1	N Marengo Ave.	N Lake Ave
717646		San Gabriel	R28.7	28.68	0.91	5+1+1	N Sunny Slope Ave.	N Kinneloa Ave
761206		Irwindale	R38.009	38.3	0.5	4+1/(1)+1	I-605 to I-210 E Off ramp	N Irwindale Ave

The EB traffic enters the network at Orange Grove Blvd and leaves the network at N Vernon Ave (Figure 1). Table 1 shows the layout of various network sections with lane configurations and milepost positions. Throughout the test bed, the number of lanes varies in different sections. Depending on the configuration of the lanes, an incident can have numerous effects on capacity. Where SR-134 starts to merge with I-210, the minimum number of lanes is four plus a HOV lane. Vehicle Detection ID 717606 (Table 1) is situated at Orange Grove Ave. near mile post R13.18. This initial section is only 0.53 miles long and has four main lanes, one HOV with no access in this section and no auxiliary lane. Similarly, the section that starts at N Marengo Ave. is almost one mile long and has an auxiliary lane along with five main lanes and one HOV lane. Here, the HOV lane still has no any entry or exit. But the last section of the study network near I-605 to I-210 off ramp has a different configuration. The auxiliary lane here starts at the I-605 to I-210 off ramp and ends at N Irwindale Ave. The whole section has four main lanes and access between the main lanes and HOV lane. Throughout the study section, the lane width varies from 11 to 12 feet. The inner shoulder width varies from 2 to 12 feet whereas the outer shoulder width remains 10 feet in most sections. The experimental case considers an incident in the EB direction just after the N Lake Ave. overpass, which has five main lanes and one HOV lane. The validation case uses different locations on the EB direction because they have available incident information. The research team places VISSIM queue counters, travel time sections and data collection stations in these sections for performance measurement. Queue counters provide average queue length, maximum queue length and number of vehicles stopped in the queue. A queue counter also measures the longest queue in the network. For both the experimental and validation cases, queue counters help identify the presence of any queue upstream of the incident during the simulation run and help calculate the queue dissipation time. A travel time section helps in the validation process where only Route 6682 of I-210 (Figure 1) is considered and it can easily measure the travel time from origin A to destination B. The data collection sections measure the microscopic level behavior such as speed, acceleration and occupancy of each vehicle in the network.

2.2. Traffic Demand

Instead of choosing an arbitrary traffic volume for the experiment, the researchers use the Caltrans PeMS database for setting likely high volume cases where an incident will result in congestion. Relying on field data for traffic demand ensures that the network performance in response to an incident reflects real conditions while the focus on peak conditions increases the importance of the incident impacts. The study uses the hourly flow data from six randomly selected months in 2006 to identify the peak hour and peak flow rate for each day of the week. For the weekday cases, the peak hour occurs at either 8:00 AM or 5:00 PM. For example, the most frequently occurring peak hour (mode) for Friday is 8:00 AM and the average peak hour flow rate for the EB direction is 5486 vehicles/hr. This study considers both Tuesday and Friday peak demands to see if a moderate change in demand during the peak hour impacts the macroscopic performance measures during an incident. The following tables give both EB and WB demands.

TABLE 2 Weekly Average Peak Hour Flow a. EB flow (left), b. WB flow (right)

Days	Time of Day	Average Hourly Flow
Friday	8	5486
Saturday	12	4917
Sunday	13	4478
Monday	17	5725
Tuesday	17	5887
Wednesday	17	5853
Thursday	17	5756

Days	Time of Day	Average Hourly Flow
Friday	8	5946
Saturday	12	5715
Sunday	13	5739
Monday	17	6043
Tuesday	17	6283
Wednesday	17	6211
Thursday	17	6186

2.3. Incident Lane Blockage (Closure)

Like traffic demand, the incident magnitude or number of affected lanes also impacts the congestion level. Due to lane drops and auxiliary lanes (Table 1), different sections of I-210 in the study test bed have different lane configurations; however, the minimum number of lanes is five. Throughout the experimental design, only main lane movements (four lanes) may be blocked by an incident while the HOV lane remains clear for all experimental trials. The researchers investigate the resulting impacts from nine different lane closure patterns. These include single lane closures for each of the four lanes and combination lane closures for contiguous lanes (e.g. lane 1 & 2, lane 2 & 3, lane 3 & 4, lanes 1-3 and lanes 2-4). Larger incidents require more lane changes and may cause the variation in performance between the different VISSIM models to increase. For validation purpose, three main lane movement and three HOV movements are considered and HOV lane movement is restricted for the HOV class type vehicles that have a passenger occupancy of more than two.

2.4. Incident Duration

The duration of any type of incident also has an effect on the network performance because longer lasting incidents typically cause longer queues to develop. All of the experimental variables discussed to this point affect the incident's impact on the network. The impact becomes more severe as the demand, the number of affected lanes and the incident duration increase. An initial review of the California PeMS data indicates that even short incidents typically last thirty minutes; therefore, the experiment considers two incident durations of thirty and forty-five minutes representing relatively typical short incidents.

Figure 2 describes different combinations for the experimental variables in each simulation trial. Incident location is the highest level in this hierarchy. Two different traffic demands for Friday (5,486) and Tuesday (5,887) represent the next experimental dimension. The nine different lane closure combinations and two incident durations (30 and 45 minutes) represent the remaining experimental dimensions. In total, these create thirty-six different experimental trials.

FIGURE 2 Variation of experimental combinations.

2.5. Parameter Mapping

The parameter comparison (Table 3) provides evidence that the default VISSIM parameters in the uncongested condition are different from the I-210 West parameters, which have been calibrated based on congested conditions. After the test bed construction, the research team selects three different sets of microscopic driving behavior parameters for the experiment. The default VISSIM parameters represent the parameters calibrated under uncongested conditions. Two other sets of driving behavior parameters represent VISSIM calibrations under congested conditions (Sheu, 2013 and Gomez *et al*., 2004). As an example of parameter mapping from earlier studies, the minimum safety distance, which Sheu (2013) describes in terms of vehicle length and standstill distance, is related to the standstill distance in the VISSIM model. The research team matches this and other similar parameters from the previous research with closely related VISSIM driver behavior parameters (those mentioned in Table 3) and generates the corresponding value for each of them. In VISSIM, different road classes have default parametric values. For the freeway section, only the highlighted parameters are changed for the Sheu and I-210 experimental models.

TABLE 3 Comparison of Calibrated Parameters

Driving Behavior Parameter Sets	Default VISSIM	Sheu [14]	I-210 [5]
Lane change (ft)			200-1450
Maximum deceleration for own (ft/s^2)		-23.95	
Maximum deceleration for the trailing vehicle ft/s^2			
Waiting time before diffusion (s)			
Safety distance reduction factor			
CC0 (Standstill distance) (ft)	4.92	3.94	5.57
CC1 (Headway time) (s)	0.9		0.9
CC2 (Following variation) (ft)	13.12		13.12
CC3 (Threshold for entering following)	-8		-8
CC4 (Negative following threshold)	-0.35		-2
CC5 (Positive following threshold)	0.35		2
CC6 (Speed dependency of oscillation)	11.44		
CC7 (Oscillation Acceleration)	0.82		
CC8 (Standstill Acceleration)	11.48	11.68	
CC9 (Acceleration at 50 mph)	4.92	7.28	

2.6. Experimental Design

The study uses three types (uncongested, congested/macro and incident/micro) of calibrated VISSIM models for the experimental test bed; for each type, variations are also evaluated based on the ranges of observed parameter values. The calibrated VISSIM model for I-210 is the base congested/macro model while the default VISSIM model serves as the uncongested model. For each "experimental incident," the study compares the three VISSIM model results. Figure 2 describes the experimental variables for each simulation trial, which is replicated for each VISSIM model. Section 3 discusses the measures included in this comparative analysis in detail.

2.7. Simulation Evaluation

This study uses two simulation output files, Data Collection and Network Performance. As its name indicates, the Network Performance output file describes network performance of the test bed. This file provides macroscopic parameters such as average speed, total delay, and total travel time. Queue counters and detectors are placed at various section of the test bed alongside with travel time sections. The queue counter output files provide the data for calculating the queue dissipation time. Travel time Station 16 is placed at the starting point of Route 6682 (Foothill Freeway, EB I-210-Segment 1). This station measures the time required for the vehicles to reach the end of this section.

3. MACROSCOPIC MEASURES OF EFFECTIVENESS

Each experimental case generates critical macroscopic performance measures like delay, travel time and speed. These measures are used for comparative analysis and validation. The research investigates differences in macroscopic performance due to changes in microscopic travel behavior and the experimental variables. One measure, Travel Time Index, is the ratio of the actual average travel time to free flow travel time. A lower index value shows better network performance and less incident impact.

Figure 3 compares four different combinations of average speed from the experiment. The left two graphs compare the speed for a 30 minute incident for different driving behavior parameters. In both cases, the macroscopic congested parameters result in lower average speed. In most cases, Sheu's microscopic congested parameters give a higher average speed than observed for the other cases. The same pattern is also found for the 45 minute incident.

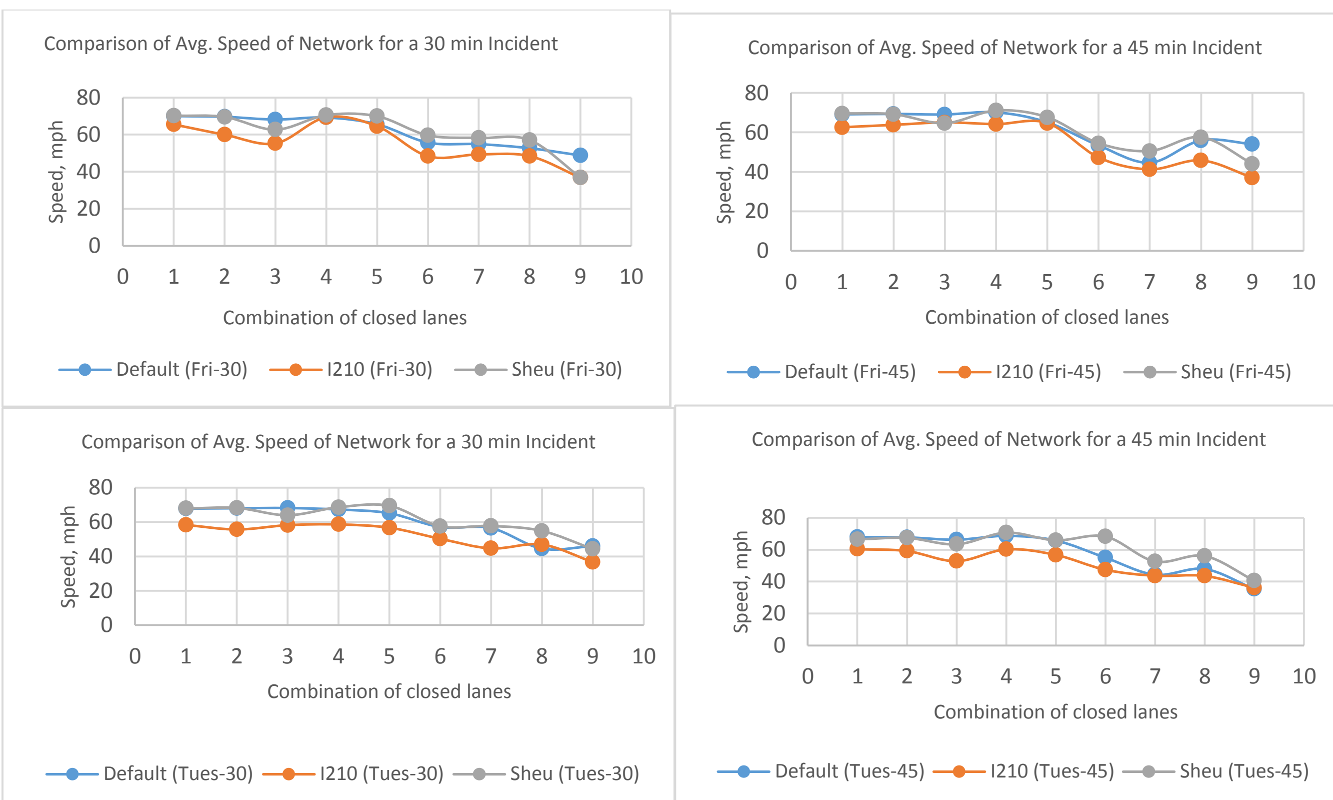

FIGURE 3 Average speed for different lane closure combinations and incident duration.

For the experimental incident location, the study also examines (Figure 4) the travel time for the 30 minute and 45 minute duration incidents with two different traffic demand and various lane closure combinations. As expected, the travel time increases with the increase in number of lanes affected by the incident; however, as incident impact increases (more lanes closed and longer time to clearance), the simulated models show greater variability. The travel time results reflect the speed results where the macroscopic parameters give a longer travel time and the microscopic parameters give a lower travel time. The network speed and total travel time charts show that the default parameters give a total travel time that lies between the I-210 and Sheu parameters. The reason behind this could be the more accurate replication of the situation in the Gomes *et al*. model because in the general case an incident induced calibrated parameter should result in lower speed than the default parameters. The comparison of travel time for a 30 minute long incident (see Figure 5) indicates that the incident duration has a significant impact on network performance.

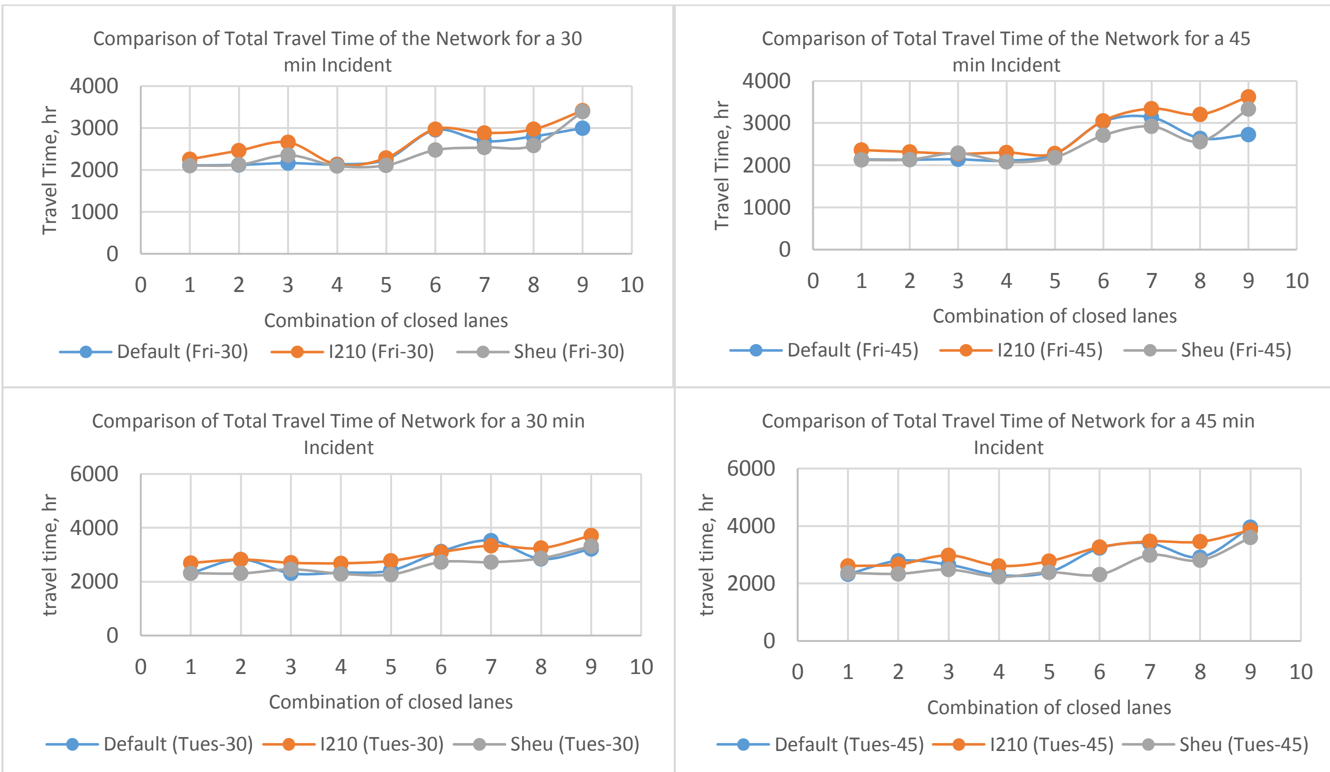

FIGURE 4 Total travel time for lane closure combinations and incident duration.

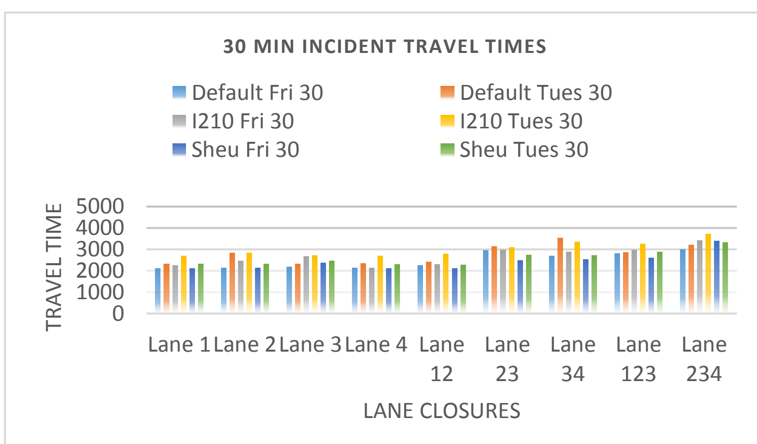

FIGURE 5 Travel time comparison for a 30 minute incident.

The percentage of difference is the ratio of the difference (non-zero) of the default value and the two congested parameter cases. The results in Table 4 show that Sheu's calibrated parameters have a smaller difference from the default for speed. For the single lane closures, all of the differences for the Sheu model remain eight percent or lower. In contrast, the I-210 model has differences in excess of twenty percent and over half of the single lane closure experiments result in differences in excess of ten percent. Sheu's model departs further from the baseline model when more lanes are closed and longer incidents occur while the I-210 model does not appear to show the same if any change in speed difference when the incident increases in size.

TABLE 4 Percentage Difference in Travel Time Measurement

Calibration		Demand	Incident Length	Lane 1	Lane 2	Lane 3	Lane 4	Lane 12	Lane 23	Lane 34	Lane 123	Lane 23
Absolute Percent error	I210	Friday	30	6.9%	16.1%	22.8%	0.2%	1.6%	0.7%	7.3%	6.1%	13.9%
		Friday	45	10.4%	8.6%	6.1%	9.2%	0.6%	0.7%	6.6%	21.3%	32.8%
		Tuesday	30	16.2%	0.1%	17.0%	14.8%	14.8%	0.9%	5.4%	14.1%	15.6%
		Tuesday	45	12.5%	4.7%	12.2%	14.1%	15.8%	1.1%	2.0%	18.4%	2.5%
	Sheu	Friday	30	0.3%	0.1%	8.6%	1.8%	6.2%	16.3%	5.6%	7.7%	13.1%
		Friday	45	0.7%	0.2%	6.8%	1.3%	3.7%	10.8%	6.8%	2.9%	22.3%
		Tuesday	30	0.1%	18.4%	6.5%	1.9%	6.2%	12.6%	22.7%	0.8%	3.2%
		Tuesday	45	2.2%	16.3%	6.5%	2.8%	0.2%	28.5%	12.0%	3.8%	9.0%

4. VALIDATION
4.1 Approach
The validation procedure compares the simulation outcomes with the field values of network performance during actual incidents on a selected set of measures of effectiveness. The observed incident impact can be assessed using macroscopic Caltrans PeMS data to generate the observed measures of effectiveness.

Failed detectors represent a common problem that research studies face while using detector data. Large quantities of data is readily available from California Performance Measurement System and the reliability of these data is pretty high. For validation, the reliability of the Vehicle Detector Stations (VDS) remain above 85% for the three different incident days (Table 6), which indicates that the field results remain relatively valid.

TABLE 6 Percent of the PeMS Detectors Working

Detectors Working			
	June 1 2014	June 9th 2014	June 30th 2014
Working	87.1	95.16	93.55
Not Working	12.9	4.84	6.45
Total	100	100	100

The simulation results can be compared to the field data during the observed incidents. For each selected performance measure, an error indicator evaluates the relationship between the simulation output and the field data. Root mean square error (RMSE) measures this divergence.

$$RMSE = \sqrt{\frac{1}{n}\sum_{i=1}^{n}(y_i - \hat{y}_i)^2} \tag{1}$$

Where $y_i =$ is the observed value of the ith observation and
$\hat{y}_i =$ is the predicted value of the ith observation

Considering the field observation as the observed value, the RMSE can be used as a measure of the spread of the y values. Mean absolute percentage errors (MAPEs) can be used to study simulated traffic arrivals, average arrival speed, and lane changing fractions. The MAPE is defined as follows:

$$MAPE = \frac{100}{N} * \sum_{i=1}^{N}\left|\frac{x_i - \hat{x}_i}{x_i}\right| \tag{2}$$

Where $x_i =$ is the field observation
$\hat{x}_i =$ is the modeled or simulated observation, and
$N =$ is the number of data points

4.2 Validation Sub-Network and Incident Description

Travel time along a segment of the network can be accumulated from the California PeMS; PeMS designates a segment of I-210 as Route 6682 (4.568 miles) and tracks travel time for this segment. The absolute start Post Mile of Route 6682 is 24.980 and the end Post Mile is 29.548. For this route, the study collects field data from three Vehicle Detection Stations (Figure 6). These stations are selected arbitrarily on the I-210 EB corridor (Route 6682-Foothill Freeway, EB, Segment 1) where incidents have occurred in real life. One downstream station captures the traffic conditions beyond the incident, which shows the number of vehicles departing the incident area. Another one is less than one mile upstream and captures the nearby incident impact. The final one is located almost at the beginning of the study section to track the number of vehicles entering the study section and calculate freeway demand; it should be in a location where the incident queue will not reach it. The study collects PeMS flow and speed measurements for these three locations every five minutes after the incident occurs.

FIGURE 6 VDS position for data validation cases.

The validation process considered six recent incidents, three HOV and three main lane, within Route 6682. The first incident, a stalled vehicle, blocked the HOV lane at Altadena (I-210 –E CA PM 28.40) on Friday, May 2, 2014, at 14:48. After being assigned at 14:57, the California Highway Patrol (CHP) cleared the incident in 26 minutes. The second HOV incident, tire debris, occurred at the same location on Friday, May 16, 2014, at 15:55 PM and lasted about 12 minutes. The last HOV incident, a metal basket in the lane, occurred near Altadena (I-210-E CA PM 29.00) on Friday, June 6, 2014, from 11:30 to 11:42. None of the HOV incidents involved a crash; however, they could still have an impact on network performance.

The remaining three incidents occurred on the main lanes. The first incident, a stalled car, occurred in lane one on Sunday, June 1, 2014 at 14:30 near I-210 –E CA PM 28.30 and required almost six minutes to clear. The second incident, tire debris blocking lane 3, took place at I-210 –E CA PM 28.40 from 6:00 to 6:26 in the morning on Monday, June 9, 2014. The last incident, plywood blocking lane three, occurred at I-210 – E CA PM 28.40 from 11:08 to 11:16 on Monday, June 30, 2014.

While none of these incidents involve crashes, they represent typical incidents that may regularly occur on any freeway. If a congested calibration reflects observed field conditions more closely for these incidents, larger incidents appear likely to magnify this importance. Table 7 summarizes the validation incident time and location data.

TABLE 7 Incident Location, Time and Duration

Date	Time of Occurrence	Duration (min)	Location	Travel Time (min)
5/2/2014	2:48:00 PM	26	HOV	14.3356
5/16/2014	3:55:00 PM	12	HOV	19.6648
6/1/2014	2:30:00 PM	6	Lane 1	4.0996
6/6/2014	11:30:00 AM	12	HOV	4.4616
6/9/2014	6:00:00 AM	26	Lane 3	4.0268
6/30/2014	11:08:00 AM	8	Lane 3	4.2428

The demand varies during each of these incidents, and PeMS data, shown in Table 8, reflects this demand. Vehicles enter the sub-network in three locations. EB I-210 Ramp enters from South Bound I-210 while the US-134 main lane movement occurs at the start of Route 6682. The US-134 HOV demand is either calculated from the US-134 main lane movement or collected from PeMS. The American Community Survey (2012) identifies that 11.09 percent of California workers over age 16 use the HOV lane. Due to the lack of HOV PeMS data, the validation sets the HOV demand for the HOV incidents at eleven percent of main lane demand.

Table 8 Validation Demand

Location	HOV 05022014	HOV 05162014	HOV 06062014	Main 06012014	Main 06092014	Main 06302014
EB I-210 Ramp	1320	1380	1080	603	150	575
US-134 HOV	560	589	536	612	120	420
US-134 Main	5088	5357	4872	4500	3000	4800

4.2 Results

The research team creates travel time sections along route 6682 (starts at O and ends at D on Figure 6) so that the simulation travel times may be directly compared with the PeMS travel times. The simulated sub-network travel times and field data appear in Table 9. For the three main lane incidents, which do not appear to have much impact on traffic conditions based on the small changes in field travel times, the three parameter sets exhibit similar performance; the simulated differences remain six percent or less. The percent error from the field conditions remains thirteen percent or less, too. The HOV incidents, which have a more pronounced impact on field conditions, see a significant difference in the simulated results. For the HOV incidents, the macroscopic congested parameters consistently estimate longer travel times which more closely reflect field conditions. While the simulated results fail to capture the full impact of the first two HOV incidents, the macroscopic congested parameters recognize that significant congestion likely occurs. For the same cases, the other parameter sets reflect travel times at least sixteen percent lower than I-210 parameters these differences increase to as much as fifty-eight percent for the second incident. The differences with the field conditions appear even more pronounced they range from nineteen to eighty percent. The validation shows that a model calibrated to capture congested conditions will produce a more accurate representation of network performance during incident conditions.

TABLE 9 Travel Time Validation

	HOV 05022014	HOV 05162014	HOV 06062014	Main 06012014	Main 06092014	Main 06302014
Field TT (min)	14.336	19.665	4.462	4.100	4.027	4.243
Default(min)	3.766	3.808	3.614	3.724	3.516	4.088
I-210(min)	8.387	9.117	4.309	3.722	3.562	4.058
Sheu (min)	4.089	3.969	3.632	3.686	3.518	3.843

The RMSE and MAPE (Table 10) reflect similar conclusions. The macroscopic congested parameters have a lower RMSE and MAPE than the other two parameter sets. The congested model appears much more capable of capturing the true impacts of congested conditions than the other two models. Sheu's model reflects the largest error because it estimates faster speeds as the typical conditions.

TABLE 10 Simulated vs. Observed RMSE and MAPE

Simulation Parameter Set	RMSE	MAPE
Default	0.535	11.1
I-210	0.323	7.13
Sheu	0.565	12.7

5. CONCLUSIONS and RECOMMENDATIONS

This study examines simulation results for three different parameter sets (uncongested, macroscopic congested and microscopic congested) during incident conditions. When comparing the results during the experimental incidents, the macroscopic congested parameter set consistently predicts longer travel times and lower speeds. The differences between the model results appear to increase as the incident magnitude increases (i.e. more lanes closed and longer clearance time); the microscopic congested parameter set exhibits a greater departure from the uncongested results as the magnitude increases. Due to the high volumes used in this study, the incident duration and number of lanes closed have a significant impact on network performance. The results indicate that the model likely has a significant impact on network performance during incident conditions and these differences become more important for larger incidents.

The second part of the study compares the same microscopic simulation parameter sets with observed field conditions inside the study network during actual incidents. For this case, the macroscopic congested parameters reflect field conditions much closer than the other parameter sets during significantly congested conditions and generate similar results with the other models during the relatively uncongested incidents. While the macroscopic congested parameters outperform the other parameter sets during congested conditions, they still fail to adequately capture incident impacts; this indicates the need to consider congested lane changing and lateral spacing behavior to capture the full incident impact. Lane changing behavior can significantly change the queue accumulation in a heavily congested network and hence additional parameter mapping appears necessary. Incident conditions also introduce the concept of compulsory lane changing maneuvers where vehicles upstream of an incident site must vacate all blocked lanes. The macroscopic parameters have a larger standstill distance, which may reflect Knoop *et al*.'s findings that the driver reaction time increases during an incident. Curiously, the microscopic congested parameter set shows the greatest departure from field conditions however, this may reflect the challenge of mapping one microscopic model into another model rather than its actual performance. This issue needs to be explored more closely by using microscopic data to directly calibrate VISSIM parameters. The study shows that a model calibrated to capture congested conditions produces a more accurate representation of network performance during incident conditions and it likely suffers little degradation in performance during uncongested conditions.

Additional future research should explore if the increase in reaction times near an incident translates to the opposing flow direction, and identify the parameters necessary to adequately capture the rubbernecking phenomenon. An ideal experiment will explore numerous sites where both site specific congested and uncongested calibration occurs; furthermore, an increase in the field cases to cover a wider range of lane closures, incident durations and demands appears valuable, too. For validation purposes, incorporating the observed O-D pattern and all network components appears critical because they can help mitigate the incident impacts; these rely on the location of the HOV's intermittent barrier and on- and off-ramps.

REFERENCES

1. Kwon, J., M. Mauch, and P. Varaiya. The components of congestion: delay from incidents, special events, lane closures, weather, potential ramp metering gain, and excess demand. In *Proceedings of the 85th annual meeting of the Transportation Research Board*, Washington, 2006.
2. Gomes, G., A. May, and R. Horowitz. Calibration of VISSIM for a Congested Freeway. *California PATH program*, Institute of Transportation Studies, California, 2004.
3. Knoop, V.L., Van Zuylen, H.J. and Hoogendoorn, S.P. Microscopic traffic behaviour near Incidents, In *Proceedings of Second Sino-Dutch Joint Workshop in Transportation and Traffic Study*, Shanghai, China, 2009.
4. Woody, T., *Calibrating Freeway Simulation Models in VISSIM. Master's Thesis Report, 2006.* http://courses.washington.edu/cee500/VISSIMCalibration_FinalReport.doc
5. Sheu, J. B., Microscopic Traffic Behavior modelling and Simulation for lane-blocking arterials incidents. *Transportmetrica A: Transport Science*, Vol. 9, No. 4, 2013, pp. 335-357.
6. Fellendorf, M., and P. Vortisch. Microscopic Traffic Flow Simulator VISSIM. Fundamentals of Traffic Simulation, International series in Operational Research and Management Science 145, DOI 10.1007/978-1-4419-6142-6_2, 2010
7. Mai *et al.* Protocol for VISSIM Simulation. Oregon Department of Transportation, 2011. www.oregon.gov/ODOT/TD/TP/APM/AddC.pdf

8. Santhanam, S. and P. Byubgkyu., Development of VISSIM Base Model for Northern Virginia (NOVA) Freeway Systems. Center for Transportation Studies at the University of Virginia, Research Report No. UVACTS-13-0-124, 2008.
9. Panwai, S., and D. Hussein. Comparative Evaluation of Microscopic Car-Following Behavior. IEEE Transactions on Intelligent Transportation System, Vol. 6, No. 3, 2005, pp. 314-325.
10. Means of Transportation to Work by Selected Characteristics for Workplace Geography. 2012 American Community Survey 1-Year Estimates. S0804. U.S. Census Bureau. http://factfinder2.census.gov/rest/dnldController/deliver?_ts=425214164750
11. Gipps, P. G., A Model for the Structure of Lane-Changing Decisions. Transportation Research Board, Vol. 20B, No. 5, 1986, pp. 403-414.
12. Hidas, P. Modelling lane changing and merging in microscopic traffic simulations. In Transportation Research Part C 10, 2002, pp. 351-371.
13. Google Map. https://www.google.com/maps/@34.142023,-118.0593021,9680m/data=!3m1!1e3
14. Hidas, P. Modelling Vehicle Interactions in Microscopic Simulation of merging and weaving. In Transportation Research Part C 13, 2005, pp. 37-62.